Hindawi Publishing Corporation
Journal of Optimization
Volume 2013, Article ID 989135, 8 pages
http://dx.doi.org/10.1155/2013/989135

*Research Article*

# Particle Swarm Optimization for Multiband Metamaterial Fractal Antenna

**Balamati Choudhury, Sangeetha Manickam, and R. M. Jha**

*Centre for Electromagnetics, CSIR-National Aerospace Laboratories, Bangalore 560017, India*

Correspondence should be addressed to Balamati Choudhury; balamati@nal.res.in

Received 27 February 2013; Accepted 2 April 2013

Academic Editor: Ling Wang



The property of self-similarity, recursive irregularity, and space filling capability of fractal antennas makes it useful for various applications in wireless communication, including multiband miniaturized antenna designs. In this paper, an effort has been made to use the metamaterial structures in conjunction with the fractal patch antenna, which resonates at six different frequencies covering both C and X band. Two different types of square SRR are loaded on the fractal antenna for this purpose. Particle swarm optimization (PSO) is used for optimization of these metamaterial structures. The optimized metamaterial structures, after loading upon, show significant increase in performance parameters such as bandwidth, gain, and directivity.

## 1. Introduction

The non-integral dimensions, recursive irregularity, and space filling capability of fractal antennas make it useful for various applications in wireless communication including miniaturized antenna designs [1]. Their property of being self-similar in the geometry leads to antennas of compact size with simplified circuit designs. Antennas, which have fractal geometry, are self-iterative, exhibiting multiband operation. Fractal antennas are frequency independent and have schemes for realizing low sidelobe designs. An antenna with fractal geometry is preferred to conventional antenna designs due to the iterative behavior of the structure, which is believed to improve the performance factors like gain, bandwidth, return loss and frequency of operation [2].

Metamaterials are artificial structures designed by placing electromagnetic (EM) resonators, such as split ring resonators (SRRs), at regular intervals. The metamaterials have frequency selective response and exhibit unique EM properties such as negative permittivity and permeability, artificial magnetism and negative refractive index, which can be used to improve the performance of antenna [3]. The media composed of metamaterials have tunable effective material parameters, and their electromagnetic response can be adjusted in real time. By using metamaterials as substrates or superstrates for antenna, significant improvements have been observed in the properties of the fractal antenna.

In this paper, an effort is made to use the square *split ring resonator* (SRR) in conjunction with the fractal patch antenna to enhance the directivity, gain, voltage standing wave ratio (VSWR), and bandwidth at multiple resonant frequencies. To serve this purpose, two different types of tunable multiband micro-split metamaterial square SRR are loaded on the fractal antenna [4]. Such an application requires design of the loaded structure at the desired frequency range (equivalent to the resonant frequencies of the fractal antenna, whose performance is to be improved). Towards this, a PSO optimizer is developed, which yields structural parameters at a particular resonant frequency. Particle swarm optimization (PSO) is an evolutionary computational technique based on the movement and intelligence of swarms, which is used for optimizing difficult multidimensional discontinuous problems in a variety of fields including electromagnetics [5, 6]. The optimal structural parameters of square SRR such as length, width, distance between successive rings for a particular resonant frequency are obtained using this efficient optimization technique based on an equivalent circuit analysis.

## 2. Overview of Metamaterial Fractal Antennas

The term fractal was first coined by Mandelbrot in 1975, in which rough, irregular, or fragmented geometric shape could be subdivided in parts, each of which was reduced-size copy of the whole [7]. A fractal antenna possesses two properties, namely, self-similarity and space filling, and hence the resonance takes place over a wide band as well as at multiple frequencies. These properties of the fractals can be used to develop new configurations for antennas and antenna arrays. Since the fractal antennas are multi-resonant and smaller in size, they are used for wireless applications. Fractal antenna can be designed to receive and transmit over a wide range of frequencies using the self-similar property associated with fractal geometry structures [2]. Space filling fractal geometries such as Hilbert curves are used to design miniature antennas, high-directive radiators, and high-impedance surfaces. This concept was used for design of miniaturized inverted-F antenna for wireless sensor networks [8]. The overall size of the antenna was reduced to 77% by using Hilbert geometry, instead of conventional rectangular patch antenna for the same resonant frequency.

Radar cross section (RCS) reduction in microstrip antenna was achieved by using Koch fractal geometry, without affecting radiation performance of the antenna [9]. An UHF Quasi-Yagi antenna surrounded by fractal metamaterial structures was designed for RFID applications. The operational frequency of this antenna was 2.4 GHz [10]. Similarly, star-shaped fractal patch antenna was used for miniaturization and backscattering radar cross-section (RCS) reduction [11]. Metamaterial unit cells could be miniaturized by incorporating fractal geometries. The effect of various geometrical parameters and the order of fractal curve on the performance of the fractal antenna were also investigated and reported that the fractal geometries of original dimensions give better performance than the miniaturized one [12].

Further, a novel negative-epsilon metamaterial was designed using fractal Hilbert curves with mirror symmetry [13]. The slotted SRRs in the ground plane were abandoned in order to reduce back radiation of the antenna. The numerical analysis and design also shows that a periodic arrangement of Hilbert curve inclusions above a conducting ground plane forms a metamaterial surface with high impedance [14].

Using multi-resonator configuration, a low-loss dispersion-optimized engineered substrate was designed for antenna miniaturization and performance enhancement. The proposed substrate contained four uncoupled inclusions with 3rd order fractal Hilbert structure. A circuit model was developed to analyze and optimize the proposed metamaterial [15]. A metamaterial with zero refractive index was designed over a wide frequency range and used as superstrate for patch antenna [16]. The designed antenna showed an antenna gain improvement by 5 dB.

It is observed from the overview of fractal antenna that Hilbert curves proved to be efficient fractal geometries to generate metamaterial surfaces. Fractal geometries were also used as miniaturized antennas with metamaterial structures as superstrate. In this paper metamaterial structures are loaded on a fractal antenna for increase in the bandwidth at the multiple distinct resonating frequencies.

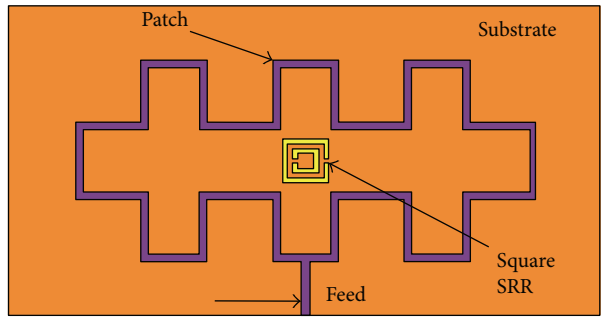


Figure 1: Top view of the square SRR loaded fractal antenna.

## 3. Design of Fractal Antenna

Fractal antennas are widely used for their compact size and light weight in wireless applications. In this work, the fractal antenna is designed with multiple resonant frequencies. Fractal patch antenna is designed on a substrate with dimensions 36 mm × 20 mm × 1.6 mm having a relative permittivity of 4.4 [17]. The patch used in the antenna layout is copper with the area 28 mm × 12 mm. The size of the patch used to feed the antenna is 0.5 mm × 4 mm. Figure 1 shows the schematic diagram of the fractal patch antenna. Further metamaterial structures are loaded on the antenna to improve the performance.

Two different algorithms, namely, PSO and bacteria foraging optimization (BFO), have been implemented towards optimization of square SRR [18]. It was observed that the execution time and accuracy of these algorithms depend on selection of parameters. For this optimization problem, the details of accuracy and execution time for both the algorithms are given in Table 1.

It is readily observed that for the class of problem in hand, PSO is highly convergent and more accurate compared to the BFO. Hence, PSO algorithm is considered in this work for further study of metamaterial antenna design.

## 4. PSO Optimization for SRR Design

The PSO is a simple, effective, and robust method used for search and optimization in various EM problems. The development of PSO can be illustrated through an analogy similar to a swarm of bees in a field. The goal of a swarm of bees in a field is to find the location with the highest density of flowers [5]. This motivates the engineers to use PSO as an optimization technique [6]. For completeness of the paper, the step-by-step algorithm is described briefly along with the flowchart (Figure 2).

*4.1. PSO Algorithm.* The PSO algorithm is given here for better understanding of the implementation for optimization of the resonant frequency (and hence extraction of the structural parameters) of a metamaterial SRR described in the following section. The step-by-step procedure is given next.

Table 1: Comparison of PSO and BFO for structural optimization of square SRR at a particular desired frequency. The substrate dielectric constant is 3.86, and desired frequency is 2.388 GHz.

| Optimization techniques | Accuracy ($f_{\text{err}}$) | Gap between rings $d$ (in mm) | Width of rings $w$ (in mm) | Length $a$ (in mm) | Execution time (in seconds) |
|---|---|---|---|---|---|
| BFO | 0.00161 | 0.12 | 0.12 | 3.96 | 12.55 |
| PSO | 0.000442 | 0.14 | 0.10 | 3.95 | 1.04 |

*Step 1.* Define the solution space. The parameters to be optimized are selected in this space. A minimum ($x_{\min(n)}$) and a maximum ($x_{\max(n)}$) range is defined, where $n$ ranges from 1 to $N$ (dimension of the optimization space).

*Step 2.* Define a fitness function. The fitness function exhibits a functional dependence that is relative to the importance of each characteristic being optimized.

*Step 3.* Initialize random swarm location and velocities. Each particle begins at its own random location with a velocity that is random in its direction and magnitude. The personal best ($p_{\text{best}}$) and the global best ($g_{\text{best}}$) are found. The personal best is the position of highest fitness locally, and global best is the position of the highest fitness of the entire swarm.

*Step 4.* Systematically fly the particles through the solution space. The algorithm acts on each particle one by one, moving it by a small amount and cycling through the entire swarm.

The following steps are encountered on each particle.

(i) Particle's fitness evaluation comparing $g_{\text{best}}$ and $p_{\text{best}}$.

(ii) Further depending on the fitness value, the particle's velocity has been updated using the following equation:

$$v_n = w * v_n + c1 * \text{rand}() * (p_{\text{best},n} - x_n) + c2 * \text{rand}() * (g_{\text{best},n} - x_n), \quad (1)$$

where $v_n$ is the velocity of a particle in the $n$th dimension; $w$ is known as inertial weight (range is between 0.0 and 1.0); $x_n$ is the particle's coordinate in the $n$th dimension; $c1$ and $c2$ are two scaling factors, which determine the relative pull of $p_{\text{best}}$ and $g_{\text{best}}$ and rand () is random function in the range [0, 1].

(iii) Once the particle velocity has been updated, the particle has to move to its next location. The velocity is applied for time-step $t$, and new coordinate $x_n$ is computed for each of the $N$ dimensions according to the following equation:

$$xn = xn + \Delta t * vn. \quad (2)$$

*Step 5.* For each particle in the swarm, Step 4 is repeated. Every second the snapshot is taken for the entire swarm, so at that time the positions of all particles are evaluated and correction is made to $p_{\text{best}}$ and $g_{\text{best}}$ values if required.

*4.2. Implementation of PSO.* Square SRR is a metamaterial structure, which consists of double square shaped ring with a gap. This structure is printed on a dielectric substrate of thickness 1.6 mm and permittivity 4.4. The schematic of a square SRR with the dimensions is shown in Figure 3, where $a$ is the side length of the square SRR, $w$ is the width of conductor, $d$ the successive distance between the rings, and $g$ is the gap present in the rings. The equivalent circuit of the square SRR is a parallel $LC$ tank circuit, given in Figure 4. The resonant frequency of the square SRR is obtained by equivalent circuit analysis method. In this method, the distributed network is converted to lumped network (Figure 4) and analysis of the resonant frequency has been carried out [19].

The resonant frequency of the split ring resonator is given by

$$f_r = \frac{1}{2\pi\sqrt{LC}}, \quad (3)$$

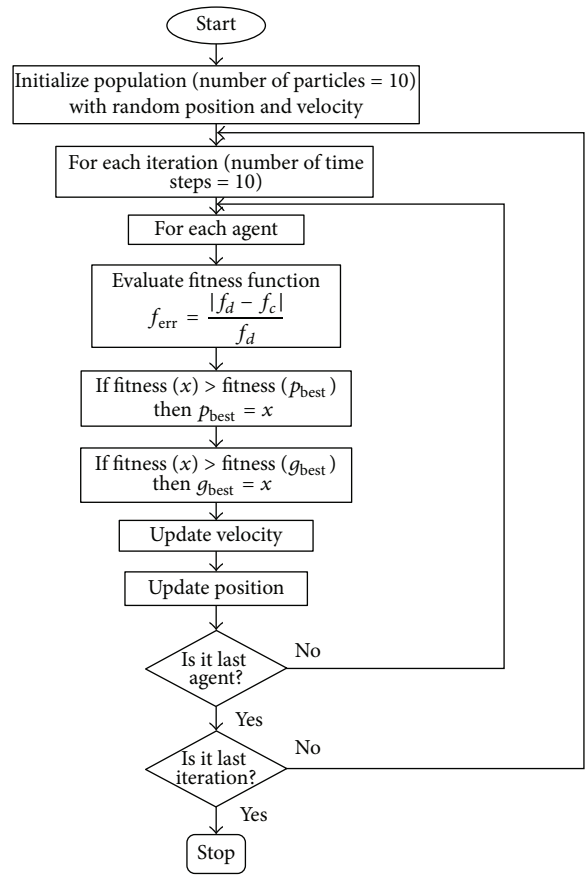


Figure 2: Flowchart of the PSO algorithm used for square SRR optimization.

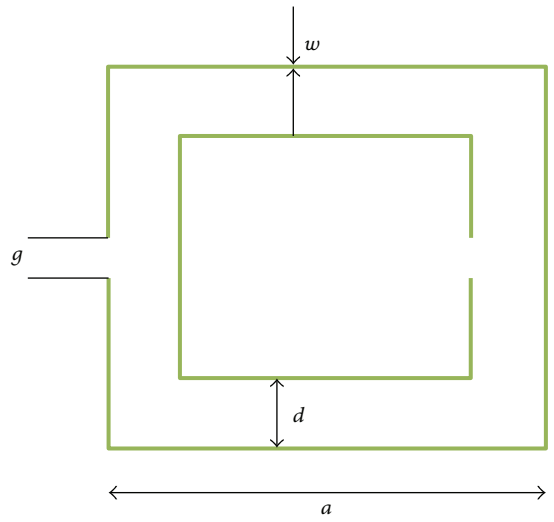


Figure 3: Top view of a unit cell of the metamaterial structure.

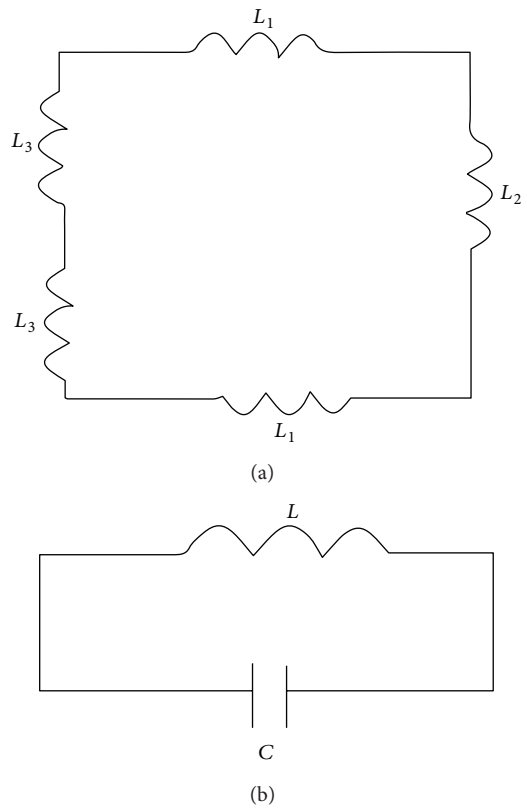


Figure 4: (a) Equivalent inductance of the square SRR. (b) Equivalent circuit of the square SRR.

where $L$ is total inductance and $C$ is gap capacitance, which are dependent on structural parameters of square SRR [20]. The expressions for $L$ and $C$ are given below.

The effective inductance of the square SRR is given by [20]

$$L = \frac{4.86\mu_0}{2}(a - w - d)\left[\ln\left(\frac{0.98}{\rho}\right) + 1.84\rho\right], \quad (4)$$

Table 2: List of parameters along with their values considered in PSO.

| PSO parameters | Value | Use |
|---|---|---|
| $w$ | 0.25 | Inertial weight |
| $c1$ | 2.05 | Constant 1, to determine $p_{\text{best}}$ |
| $c2$ | 2.05 | Constant 2, to determine $g_{\text{best}}$ |
| $N_p$ | 10 | Number of particles |
| $N_d$ | 5 | Number of dimensions |
| $N_t$ | 20 | Number of time steps |
| $X_{\min}$ | 0 | Scalar, min. for particle position |
| $X_{\max}$ | 10 | Scalar, max. for particle position |
| $V_{\min}$ | −1.5 | Scalar, min. for particle velocity |
| $V_{\max}$ | 1.5 | Scalar, max. for particle velocity |

where $\rho$ is the filling factor which depends on width and thickness of the SRR. The filling factor with respect to Figure 3 is given by

$$\rho = \frac{w + d}{a - w - d}. \quad (5)$$

Similarly, the effective capacitance is given by

$$C_s = \left(a - \frac{3}{2}(w + d)\right)C_{\text{pul}}, \quad (6)$$

where $C_{\text{pul}}$ is the per-unit-length capacitance between the rings which is given as

$$C_{\text{pul}} = \varepsilon_0\varepsilon_{\text{eff}}\frac{K\left(\sqrt{1 - k^2}\right)}{K(k)}. \quad (7)$$

Here $\varepsilon_{\text{eff}}$ is the effective dielectric constant, which is expressed as

$$\varepsilon_{\text{eff}} = \frac{\varepsilon_r + 1}{2}. \quad (8)$$

$K(k)$ denotes the complete elliptical integral of the first kind with $k$ expressed as

$$k = \frac{d}{d + 2w}. \quad (9)$$

The PSO optimizer acts here as a CAD package which yields the structural parameters such as the length, width, and spacing at a desired resonant frequency. The cost function used for this optimization is

$$f_{\text{err}} = \frac{|f_d - f_c|}{f_d}, \quad (10)$$

where, $f_d$ is the desired frequency and $f_c$ is the frequency arrived at by the equivalent circuit analysis. As per the algorithm mentioned, the different parameters are assigned with respect to the problem. The parameters of the PSO program are given in Table 2. The selection of PSO parameters such as $w$, $c1$, and $c2$ considered are from the original work by Kennedy and Eberhart [5]. The inertial weight is always

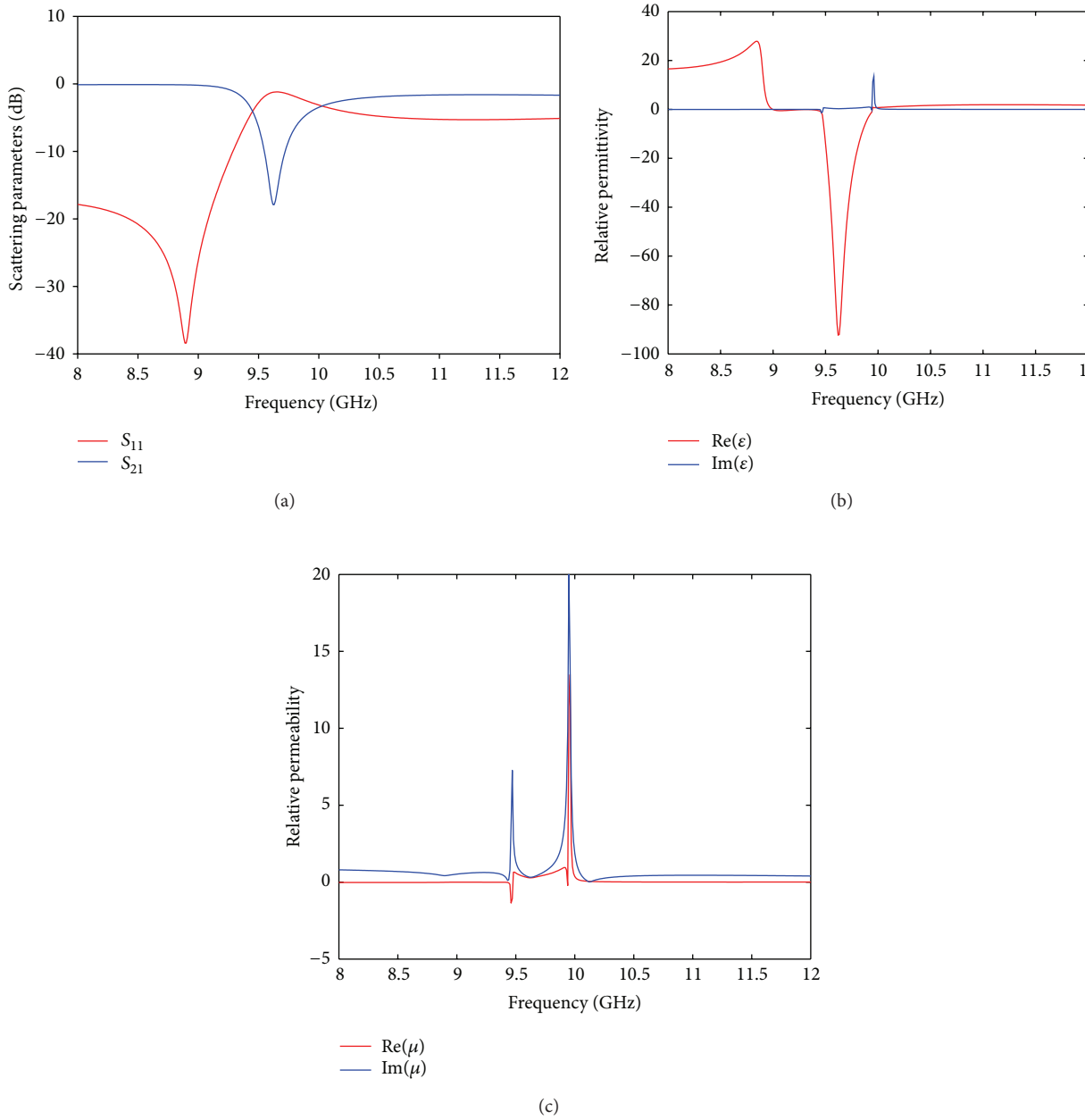


FIGURE 5: (a) Scattering parameters $S_{11}$ and $S_{21}$ parameters of the designed square SRR optimized using PSO algorithm. (b) Relative permittivity of the designed square SRR as optimized by the PSO. (c) Relative permeability of the designed square SRR as optimized by the PSO.

considered as less than one and varies with iteration [6]. The parameter $N_d$, that is, number of dimensions is taken with respect to square SRR parameters to be optimized such as $a$, $w$, $d$, $\varepsilon$, $f_{\text{err}}$. Similarly, there is no specific criteria for selection of exact values for $N_p$, $N_t$ and is generally taken by trial and error method with respect to complexity of problem [6]. $X_{\min}$, $X_{\max}$, $V_{\min}$, and $V_{\max}$ are the initial search values, which update with the iteration cycle.

The PSO optimizes the fitness function and extracts the structural parameters. The extracted length $a$, width $w$, and the space between the inner and outer ring $d$ are 2.8 mm, 0.3 mm, and 0.3 mm, respectively. These optimized values are used for the design of the square SRR, and the relative permittivity and permeability values are extracted using (5) and (6) [20].

The simulated scattering parameters ($S_{11}$ and $S_{21}$) of the square SRR placed exactly at the middle of the fractal antenna and the corresponding extracted relative permittivity and permeability are given in Figure 5(a) through Figure 5(c). The metamaterial characteristics of the proposed structure are readily inferred in Figure 5(b), from 9.35 GHz to 9.94 GHz. Similarly, Figure 6(a) shows the top view of a unit cell of the metamaterial structure with micro-splits. The scattering parameters of the second square micro-split SRR placed over

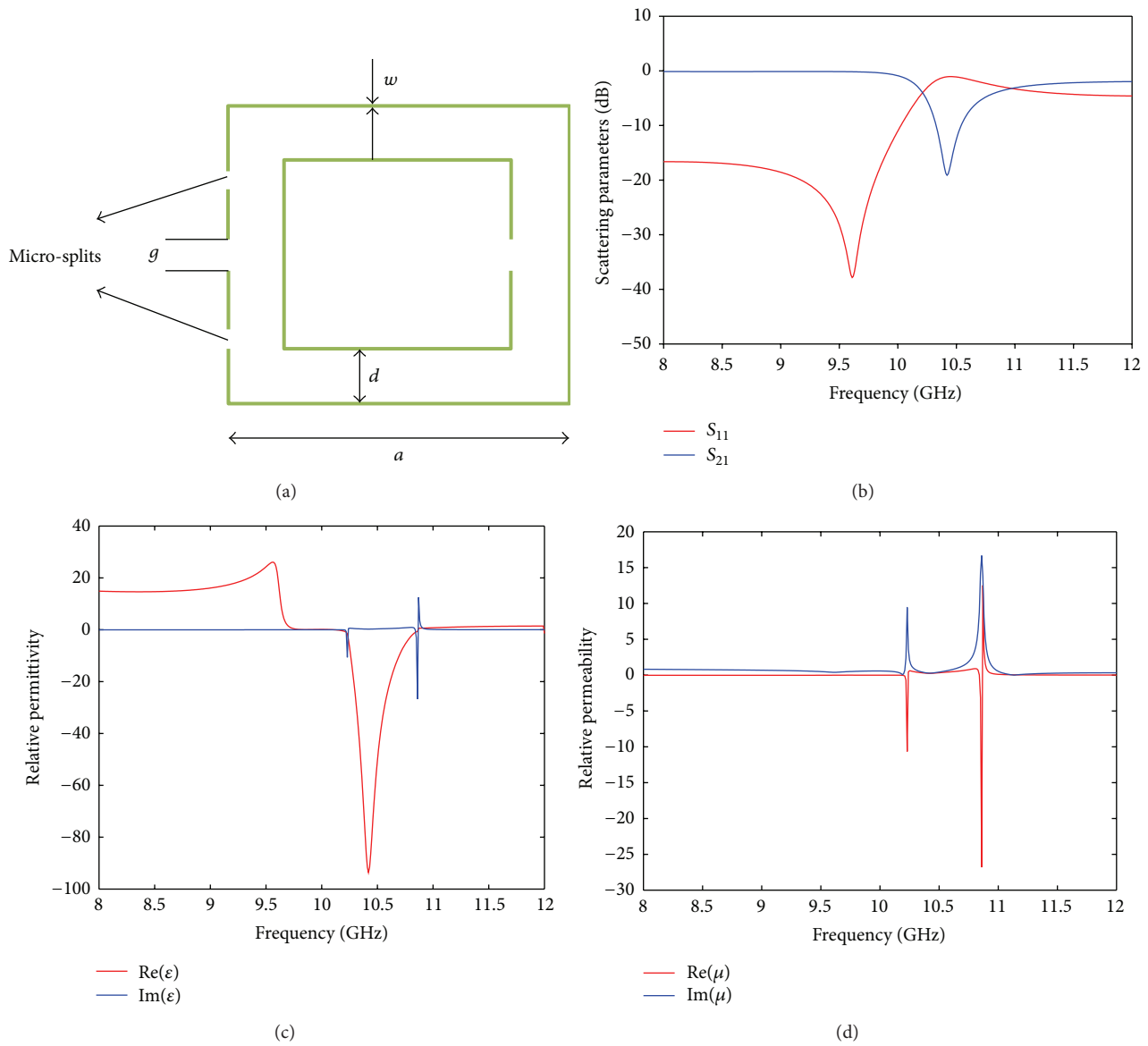


FIGURE 6: (a) Top view of a unit cell of the metamaterial structure with micro-splits (square micro-split SRR), (b) Scattering parameters $S_{11}$ and $S_{21}$ parameters of the designed square micro-split SRR. (c) Extracted permittivity of the designed square micro-split SRR. (d) Extracted permeability of the designed square micro-split SRR.

the fractal antenna and the corresponding extracted relative permittivity and permeability are shown in Figure 6(b) through Figure 6(d):

$$n = \frac{1}{kd}\cos^{-1}\left[\frac{1}{2S_{21}}\left(1 - S_{11}^2 + S_{21}^2\right)\right],$$
$$z = \sqrt{\frac{\left(1 + S_{11}^2\right)^2 - S_{21}^2}{\left(1 - S_{11}^2\right)^2 - S_{21}^2}}, \quad (11)$$
$$\varepsilon = \frac{n}{z},$$
$$\mu = nz,$$

where $w$ = radian frequency, $d$ = thickness of the unit cell.

The PSO algorithm is implemented to optimize the structural square SRR parameters such as width, length, and gap between the splits, for a desired frequency of operation with the overall objective to improve the performance characteristics of the fractal antenna.

## 5. Performance Enhancement Using Optimized Square SRR

A metamaterial square split ring resonator, whose structural parameters were optimized using particle swarm optimization, was designed and placed at the centre of the fractal patch antenna as shown in Figure 1. After loading a single optimized metamaterial square SRR, it is observed that although the performance of the antenna is increased compared to

Table 3: Characteristics of the fractal patch antenna after the addition of metamaterial structure.

| Parameters | Resonant frequency of the fractal patch (GHz) | | | | | |
|---|---|---|---|---|---|---|
| | 3.37 | 4.96 | 6.42 | 7.76 | 8.93 | 12.37 |
| Bandwidth (MHz) (without SRR) | 40 | 85 | 99.5 | 220 | 60 | 420 |
| Bandwidth (MHz) (with SRR) | 46 | 340 | 120 | 220 | 120 | 460 |
| Return loss (dB) (with SRR) | −12.50 | −31.52 | −26.8 | −20.35 | −13.30 | −21.26 |
| Directivity (dB) (with SRR) | −3.14 | 4.86 | 3.31 | 7.79 | 5.69 | 6.21 |

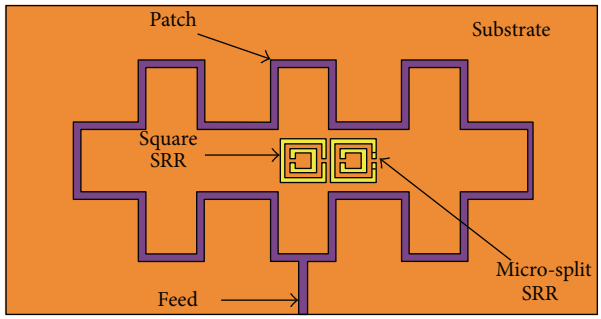


Figure 7: Two different square SRR (square SRR and square micro-split SRR) loaded in the fractal antenna elements.

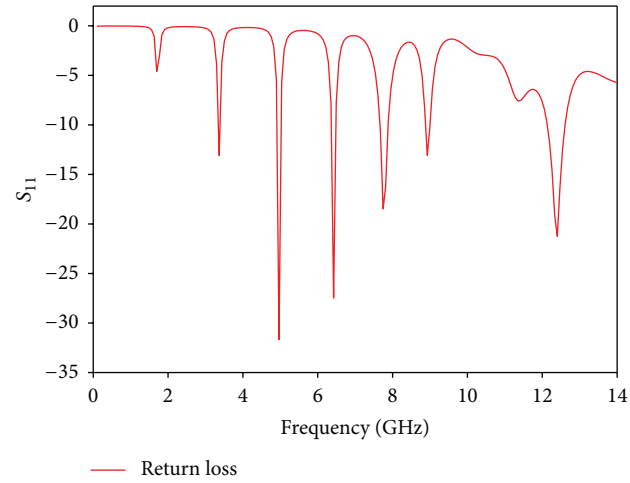


Figure 8: Return loss of the metamaterial fractal patch antenna.

the fractal patch antenna without metamaterial, it is not significant at all the resonant frequencies. Further, in order improve the performance of the fractal patch antenna at all the resonant frequencies, a square SRR with micro-splits in the outer ring is loaded in conjunction with the optimized square SRR (Figure 7). Particle swarm optimization is used for optimization of these metamaterial structures using the algorithm given in Section 4.

The micro-split in the SRR ring helps to resonate at multiple frequencies and improves multiband operation of the antenna. By using two different types of square SRR, the performance parameters of the fractal antenna such as return loss, gain, directivity, bandwidth, and VSWR are improved at multiple resonant frequencies.

The designed metamaterial fractal antenna resonates at six distinct resonant frequencies, which covers both the C and X band (Figure 8). The simulation results show that there is a significant improvement in the antenna characteristics. Table 3 shows the results after placing the metamaterial SRR with micro-splits over the fractal patch antenna.

After placing the metamaterial SRR over the fractal antenna, there is a significant decrease in the return loss and at the same time the bandwidth is widened, with enhancement in the gain and directivity. The radiation efficiency is improved to 40%. It is clearly seen that the gain and directivity of the antenna are improved. There is also an increase in bandwidth at each resonant frequency. Figures 8 and 9 show the simulation results of the fractal patch antenna with optimized metamaterial SRR and micro-split SRR at the middle of the antenna.

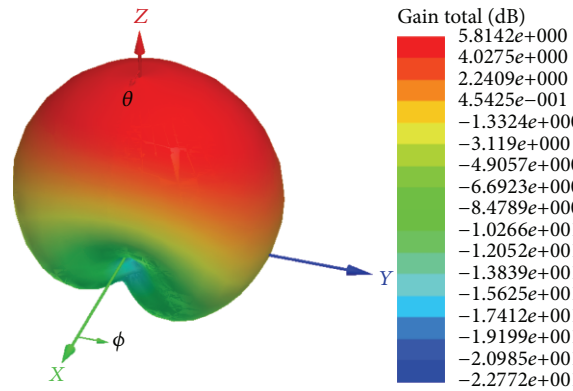


Figure 9: Radiation pattern of the metamaterial fractal patch antenna at 7.76 GHz.

## 6. Conclusion

A multiband metamaterial fractal antenna is designed and simulated, which resonates at six different frequencies covering both C and X band. Two different types of metamaterial structures, namely, a square SRR and a square micro-split SRR, are loaded at the center of the antenna. A PSO based optimizer is used to extract the structural parameters of these metamaterial structures. A comparative analysis of the fractal

antenna with and without SRR is reported. It is observed that the radiation efficiency has increased up to 40% after loading the optimized SRRs. The bandwidth at each resonant frequency increases significantly because of the square micro-split SRR. There is also a noticeable improvement in the directivity, as well as the gain at various resonant frequencies.

## References


[1] D. H. Werner, R. L. Haupt, and P. L. Werner, "Fractal antenna engineering: the theory and design of fractal antenna arrays," *IEEE Antennas and Propagation Magazine*, vol. 41, no. 5, pp. 37–58, 1999.

[2] T. E. Nur, S. K. Ray, D. Paul, and T. Mollick, "Design of fractal antenna for ultra- wideband applications," *International Journal of Research and Reviews in Wireless Communications*, vol. 1, no. 3, pp. 66–74, 2011.

[3] Y. Rahmat-Samii, "Metamaterials in antenna applications: classifications, designs and applications," in *Proceedings of IEEE International Workshop on Antenna Technology Small Antennas and Novel Metamaterials (IWAT '06)*, pp. 1–4, March 2006.

[4] E. Ekmekci, K. Topalli, T. Akin, and G. Turhan-Sayan, "A tunable multi-band metamaterial design using micro-split SRR structures," *Optics Express*, vol. 17, no. 18, pp. 16046–16058, 2009.

[5] J. Kennedy and R. Eberhart, "Particle swarm optimization," in *Proceedings of the IEEE International Conference on Neural Networks*, pp. 1942–1948, December 1995.

[6] J. Robinson and Y. Rahmat-Samii, "Particle swarm optimization in electromagnetics," *IEEE Transactions on Antennas and Propagation*, vol. 52, no. 2, pp. 397–407, 2004.

[7] B. B. Mandelbrot, *Fractals. Form, Chance and Dimension*, W.H. Freeman, Amsterdam, The Netherlands, 1977.

[8] J. T. Huang, J. H. Shiao, and J. M. Wu, "A miniaturized Hilbert inverted-F antenna for wireless sensor network applications," *IEEE Transactions on Antennas and Propagation*, vol. 58, no. 9, pp. 3100–3103, 2010.

[9] G. Cui, Y. Liu, and S. Gong, "A novel fractal patch antenna with low RCS," *Journal of Electromagnetic Waves and Applications*, vol. 21, no. 15, pp. 2403–2411, 2007.

[10] H. X. D. Araujo, S. E. Barbin, and L. C. Kretly, "Design of UHF Quasi-Yagi antenna with metamaterial structures for RFID applications," in *Proceedings of IEEE Microwave and Optoelectronics Conference*, pp. 8–11, November 2011.

[11] Y. B. Thakare and Rajkumar, "Design of fractal patch antenna for size and radar cross-section reduction," *IET Microwaves, Antennas and Propagation*, vol. 4, no. 2, pp. 175–181, 2010.

[12] V. Crnojević-Bengin, V. Radonić, and B. Jokanović, "Fractal geometries of complementary split-ring resonators," *IEEE Transactions on Microwave Theory and Techniques*, vol. 56, no. 10, pp. 2312–2321, 2008.

[13] M. Palandoken and H. Henke, "Fractal negative-epsilon metamaterial," in *Proceedings of the International Workshop on Antenna Technology: Small Antennas, Innovative Structures and Materials (iWAT '10)*, pp. 1–4, March 2010.

[14] J. McVay, N. Engheta, and A. Hoorfar, "High impedance metamaterial surfaces using Hilbert-curve inclusions," *IEEE Microwave and Wireless Components Letters*, vol. 14, no. 3, pp. 130–132, 2004.

[15] L. Yousefi and O. M. Ramahi, "Miniaturized wideband antenna using engineered magnetic materials with multi-resonator inclusions," in *Proceedings of the IEEE Antennas and Propagation Society International Symposium (AP-S '07)*, pp. 1885–1888, June 2007.

[16] J. Ju, D. Kim, W. J. Lee, and J. I. Choi, "Wideband high-gain antenna using metamaterial superstrate with the zero refractive index," *Microwave and Optical Technology Letters*, vol. 51, no. 8, pp. 1973–1976, 2009.

[17] S. Suganthi, S. Raghavan, and D. Kumar, "Miniature fractal antenna design and simulation for wireless applications," in *Proceedings of the IEEE International Conference on Recent Advances in Intelligent Computational Systems Trivandrum (RAICS '11)*, September 2011.

[18] B. Choudhury, S. Bisoyi, G. Hiremath, and R. M. Jha, "Emerging trends in soft computing for metamaterial design and optimization," in *Proceedings of the Symposium on Metamaterials, International Conference on Computational and Experimental Engineering and Sciences (ICCES '12)*, Crete, Greece, April 2012.

[19] J. W. Fan, C. H. Liang, and X. W. Dai, "Design of cross-coupled dual-band filter with equal-length split-ring resonators," *Progress in Electromagnetics Research*, vol. 75, pp. 285–293, 2007.

[20] F. Bilotti, A. Toscano, and L. Vegni, "Design of spiral and multiple split-ring resonators for the realization of miniaturized metamaterial samples," *IEEE Transactions on Antennas and Propagation*, vol. 55, no. 8, pp. 2258–2267, 2007.